



# Production of carbohydrates, lipids and polyunsaturated fatty acids (PUFA) by the polar marine microalga *Chlamydomonas malina* RCC2488

Daniela Morales-Sánchez<sup>a</sup>, Peter S.C. Schulze<sup>a</sup>, Viswanath Kiron<sup>a</sup>, René H. Wijffels<sup>a,b,\*</sup>

<sup>a</sup> Faculty of Biosciences and Aquaculture, Nord University, Bodø, Norway

<sup>b</sup> Bioprocess Engineering, AlgaePARC, Wageningen University, Wageningen, Netherlands

## ARTICLE INFO

### Keywords:

Chlamydomonas  
Salinity  
Nitrogen deprivation  
Light intensity  
PUFA  
Polar microalgae

## ABSTRACT

Polar microalgae that are highly productive in cold climates can produce large amounts of biomass and polyunsaturated fatty acids (PUFA). The polar *Chlamydomonas malina* RCC2488, grows at low temperatures and produces high amounts of lipids, which are mainly composed of PUFA. However, not much is known about its phylogenetic relationship with other strains within the order Chlamydomonadales and the optimum growth conditions for maximum biomass productivity have not yet been identified. In this study, a phylogenetic analysis was performed to determine the closest relatives of *C. malina* within the Chlamydomonadales order. To select the best growth conditions for maximum biomass productivities in cultivations performed at 8 °C, different salinities (0–80) and light intensities (70–500 μmol photons m<sup>-2</sup> s<sup>-1</sup>) were tested, using bubble column and flat-panel photobioreactors. The effect of nitrogen limitation was tested to determine if *C. malina* can accumulate energy reserve metabolites (carbohydrates and lipids). Phylogenetic analysis confirmed that *C. malina*, which belongs to the Chlamydomonadales order, is closely related to the psychrophilic *Chlamydomonas* sp. UWO 241 and *Chlamydomonas* sp. SAG 75.94, as well as to the mesophilic *C. parkeae* MBIC 10599. The highest biomass (527 mg L<sup>-1</sup> day<sup>-1</sup>), lipid (161.3 mg L<sup>-1</sup> day<sup>-1</sup>) and polyunsaturated fatty acids (PUFA; 85.4 mg L<sup>-1</sup> day<sup>-1</sup>) productivities were obtained at a salinity of 17.5, light intensity of 250 μmol photons m<sup>-2</sup> s<sup>-1</sup> and nitrogen replete conditions. Strikingly, the marine *C. malina* can grow even in fresh water, but the biomass productivity was reduced. While the intracellular lipid content remained unchanged under nitrogen deprivation, the carbohydrate content increased (up to 49.5% w/w), and the protein content decreased. The algal lipids were mainly comprised of neutral lipids, which were primarily composed of PUFA. *Chlamydomonas malina* RCC2488 is a polar marine microalga suitable for high biomass, carbohydrate, lipid and PUFA productivities at low temperatures.

## 1. Introduction

Polyunsaturated fatty acids (PUFA) have gained interest in the pharmaceutical industry due to its beneficial properties for human and animal health [1–3]. PUFA used for human nutrition are mainly obtained from fish oil [3,4]. However, obtaining PUFA from fish have several limitations, such as possible depletion of the resource, contamination with heavy metals, variability in the oil composition and quality, unpleasant odor, and environmental negative impacts like degradation of marine habitats [3–6]. On the other hand, through the food chain, fish obtain PUFA from microalgae via bioaccumulation [4,7]. PUFA from microalgae can be a sustainable, environmentally friendly, and a “vegetarian and vegan” alternative [2,8,9]. Moreover, its production can be enhanced by using polar or cold adapted microalgae, which are the ideal candidate due to its naturally occurring high

PUFA content [10]. The synthesis of PUFA in polar microalgae is induced at low temperatures because these compounds help to maintain the fluidity, flexibility, and functionality of the cellular membranes, which is a crucial adaptive strategy to support the cellular metabolism at such temperatures [9,10]. Also, polar microalgae have developed mechanisms to successfully adapt to low temperatures, oscillating light conditions, osmotic pressure, and oxidative or nutrient stresses [11–14]. Such adaptation to a wide range of environmental conditions has bestowed these microorganisms with a high degree of phenotypic plasticity [13,15], which makes them interesting organisms for the production of PUFA, and other high-value metabolites. Polar or cold-adapted microalgal species that have shown evidence of high biomass and/or PUFA productivities at low temperature include *Chlamydomonas pulsatilla*, *C. klinobasis*, *C. malina* RCC2488, *Chloromonas platystigma*, *Raphidonema sempervirens*, and *Koliella antarctica* [9,16,17].

\* Corresponding author at: Faculty of Biosciences and Aquaculture, Nord University, Bodø, Norway.

E-mail address: [rene.wijffels@wur.nl](mailto:rene.wijffels@wur.nl) (R.H. Wijffels).

<https://doi.org/10.1016/j.algal.2020.102016>

Received 8 April 2020; Received in revised form 6 July 2020; Accepted 16 July 2020

Available online 24 July 2020

2211-9264/ © 2020 The Authors. Published by Elsevier B.V. This is an open access article under the CC BY license (<http://creativecommons.org/licenses/by/4.0/>).

*Chlamydomonas malina* RCC2488 (called *C. malina* hereafter) is a polar microalga isolated in 2009 from the Beaufort Sea of the Arctic Ocean [18]. In our previous study, *C. malina* had high levels of PUFA when cultivated at 8 °C compared to 15 °C [17]. However, the phylogenetic relationship of *C. malina* within the Chlamydomonadales order and its best growth conditions for obtaining desired biomass and metabolites are yet to be investigated. In this study, we performed a phylogenetic analysis of the 18S rRNA gene sequence of *C. malina* and available *Chlamydomonas* strains. We report the performance of *C. malina* under different experimental conditions, such as salt concentrations, light intensities, and nitrogen stress, to identify the optimal growth conditions at which this microalga produces commercially important metabolites, such as lipids, carbohydrates, and PUFA.

## 2. Materials and methods

### 2.1. Strain

The polar marine microalgae *Chlamydomonas malina* RCC2488 was obtained from the Roscoff Culture Collection, France (RCC). This strain was isolated from the Beaufort Sea, within the Arctic Ocean, at latitude 69°48 N and longitude 138°26E [18]. The strain has been maintained in k/2 media at 4 °C, and transferred to fresh media every 4 weeks at the culture collection station (<http://roscoff-culture-collection.org/rcc-strain-details/2488>).

### 2.2. Phylogenetic analyses

The sequence of the 18S ribosomal RNA gene of *C. malina* strain was obtained from the Roscoff Culture Collection with accession number JN934686. 18S rRNA related genes were identified by BLASTN searches against GenBank and NCBI, using *C. malina* 18S rRNA gene sequence as a query (JN934686). Sequences were aligned by Muscle [19]; all gaps and missing data were eliminated. The evolutionary history was inferred by constructing a phylogenetic tree using the Maximum Likelihood method based on the Tamura-Nei Model [20]. Evolutionary analyses were conducted in MEGA7 [21].

### 2.3. Culture conditions

Stock cultures were maintained on agar plates containing f/2 medium [22]. Inocula for all experiments were cultured in 250 mL Erlenmeyer shake-flasks (100 rpm) containing 100 mL of f/2 at 8 °C with an irradiance of  $\sim 120 \mu\text{mol photons m}^{-2} \text{s}^{-1}$  (Phillips TLD 840 fluorescence lamps) and ambient levels of CO<sub>2</sub>. For the medium preparation, we used seawater from the North Atlantic shoreline of Bodø (Norway) containing a salinity approximately of 35. The f/2 medium comprised the following macronutrients (in mM): NaNO<sub>3</sub> 31.8, NaH<sub>2</sub>PO<sub>4</sub>·H<sub>2</sub>O 1.32, FeCl<sub>3</sub>·6H<sub>2</sub>O 0.105, Na<sub>2</sub>EDTA·2H<sub>2</sub>O 0.105, trace elements (in  $\mu\text{M}$ ): CuSO<sub>4</sub>·5H<sub>2</sub>O 0.36, Na<sub>2</sub>MoO<sub>4</sub>·2H<sub>2</sub>O 0.234, ZnSO<sub>4</sub>·7H<sub>2</sub>O 0.69, CoCl<sub>2</sub>·6H<sub>2</sub>O 0.378, MnCl<sub>2</sub>·2H<sub>2</sub>O 8.19, and vitamins (in  $\mu\text{M}$ ): thiamine HCl 26.6, biotin 0.18 and cyanocobalamin 0.036. The initial biomass concentration of all experiments was around 0.2 g of dry cell weight (DCW) L<sup>-1</sup>. For salinity experiments, *C. malina* was cultured in f/2 medium and 120  $\mu\text{mol photons m}^{-2} \text{s}^{-1}$  for 10 days at salinities 0, 17.5, 35, and 80, using combinations of fresh water (salinity: 0) and seawater (salinity: 35) or supplementing with NaCl for higher salinity (80). For testing of different light intensities and nitrogen stress, a salinity 17.5 was used. For light intensity experiments, *C. malina* was grown in f/2 medium for 10 days at 70, 120, 250 and 500  $\mu\text{mol photons m}^{-2} \text{s}^{-1}$ . For nitrogen stress experiments, *C. malina* was pre-cultured in f/2 medium and 120  $\mu\text{mol photons m}^{-2} \text{s}^{-1}$  until the middle logarithmic phase was reached (day 5). At this growth stage, cells were collected by centrifugation, washed twice with water (salinity:17.5), and re-suspended in f/2 medium with NaNO<sub>3</sub> (F2 + N) or without NaNO<sub>3</sub> (F2–N) at a biomass concentration of 1.5 g<sub>DCW</sub> L<sup>-1</sup>. The

**Table 1**

Different conditions used in the treatments tested in the present work.

| Treatment       | Salinity (-) | Light intensity ( $\mu\text{mol photons m}^{-2} \text{s}^{-1}$ ) | Nitrogen supplied | Photobioreactor |
|-----------------|--------------|--|-------------------|-----------------|
| Salinity        | 0            | 120  | +                 | Bubble column   |
|                 | 17.5         | 120  | +                 |                 |
|                 | 35           | 120  | +                 |                 |
|                 | 80           | 120  | +                 |                 |
| Light intensity | 17.5         | 70   | +                 | Flat-panel      |
|                 | 17.5         | 120  | +                 |                 |
|                 | 17.5         | 250  | +                 |                 |
|                 | 17.5         | 500  | +                 |                 |
| Nitrogen stress | 17.5         | 250  | +                 | Bubble column   |
|                 | 17.5         | 250  | -                 |                 |

+ : Nitrogen replete conditions.

- : Nitrogen deplete conditions.

nitrogen stress experiments denote the presence or absence of NaNO<sub>3</sub>, referred as only nitrogen hereafter. Cultures were grown for five days at a light intensity of 250  $\mu\text{mol photons m}^{-2} \text{s}^{-1}$ . After five days, cells were harvested by centrifugation (2000 g,  $t = 5$  min), washed with 0.5 M ammonium formate, centrifuged again (2000 g,  $t = 5$  min), and the pellets were stored at  $-70$  °C for further analyses.

### 2.4. Cultivation in photobioreactors

Salinity and nitrogen stress experiments were conducted in bubble column photobioreactors (Table 1) designed by Hulatt et al. [16]. Briefly, the arrangement consisted of glass tubes (Friedel, Oslo, Norway) measuring 35 mm internal diameter with 300 mL of working volume, fitted with sealed silicon stoppers and autoclaved as complete units at 121 °C for 20 min. The medium was autoclaved separately in 1 L flasks. Filtered air (0.2  $\mu\text{m}$ , Acrodisc® PTFE filters, Pall Corporation, USA) containing 1% CO<sub>2</sub> was supplied to each photobioreactor at a flow of 1 vvm (300 mL min<sup>-1</sup>) using a rotameter (Omega, Manchester, UK). A mass flow control system (GMS-150, Photon Systems Instruments, Czech Republic) was used to control the CO<sub>2</sub> concentration by mixing it with compressed air. These photobioreactor systems were placed in a temperature-controlled environment chamber at 8 °C (Termaks AS, Bergen, Norway) fitted with nine fluorescent lamps (cool daylight, 36 W, Phillips) illuminated from one side at a light intensity of 120  $\mu\text{mol photons m}^{-2} \text{s}^{-1}$ .

For a more uniformity of the photosynthetic photon flux density (PPFD), the light intensity experiments were carried out in autoclaved flat-panel photobioreactors (Algaemist-S, Ontwikkelwerkplaats, Wageningen UR, The Netherlands) (Table 1), fully described previously [23]. The measurement of the PPFD impinging on the front of the cultivation vessel was performed using a Li-Cor189 2 $\pi$  quantum sensor (LI-COR Biosciences, Lincoln, NE, USA), accordingly to Suzuki et al. [9]. The working volume was 380 mL with a light path of 14 mm. The cultures were aerated at 1 vvm with 0.2  $\mu\text{m}$  filtered air mixed with 1% CO<sub>2</sub>. Continuous light intensity of 70, 120, 250 and 500  $\mu\text{mol photons m}^{-2} \text{s}^{-1}$  was provided by warm-white LEDs. The cultivation temperature of 8 °C  $\pm$  0.5 °C was controlled by the Algaemist software. Initial pH was 7 without control along the cultivation period. All experiments were carried out in triplicate for 10 days.

### 2.5. Growth measurements

The growth of *C. malina* was measured by the optical density, which was calibrated against the dry weight. Samples of the culture (0.5–1 mL) were collected daily to measure the absorbance at 750 nm in a 1 cm micro-cuvette using a spectrophotometer (Hach-Lange DR3900, Hach, International). The DCW was evaluated gravimetrically by filtering 5–10 mL of culture through a pre-dried and pre-weighed

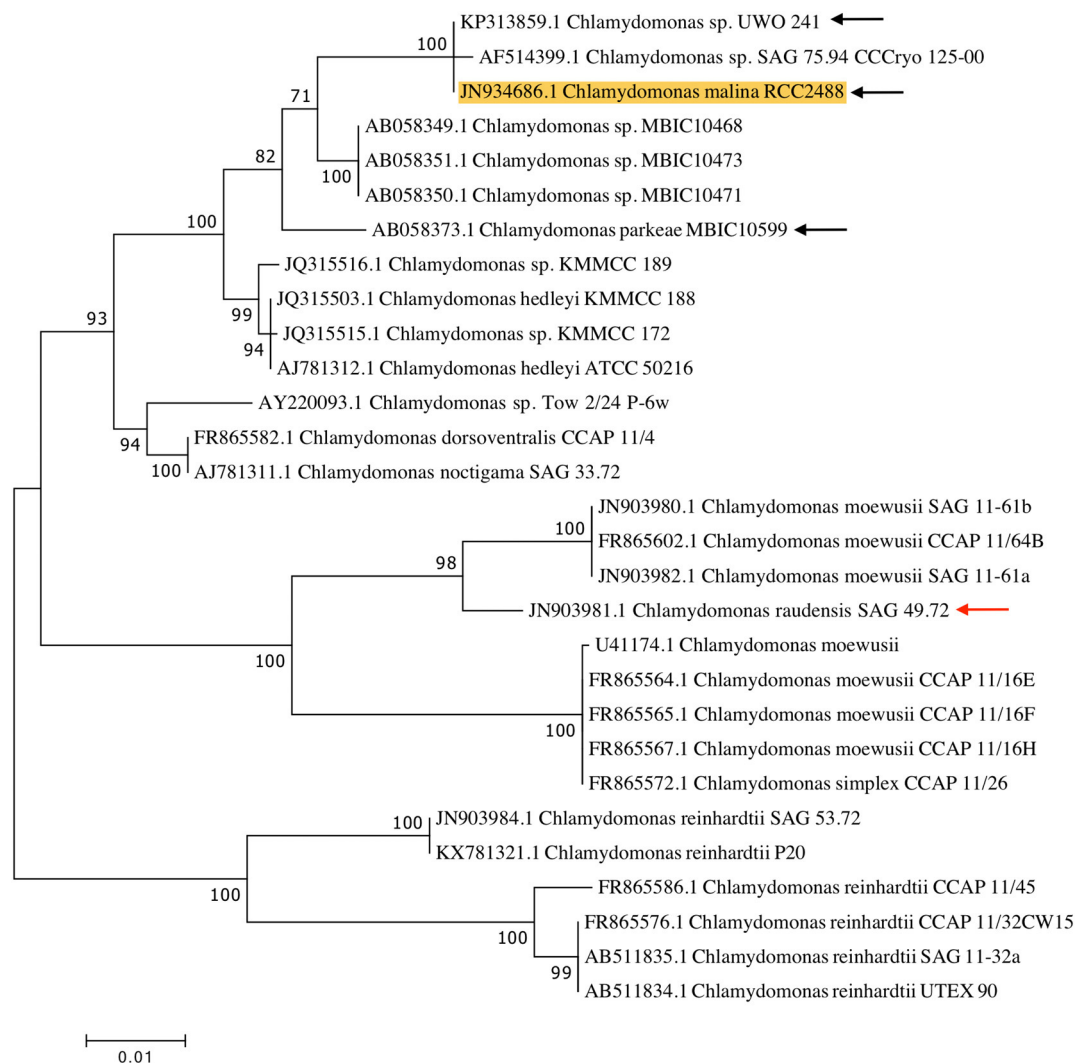


**Fig. 1.** Phylogenetic tree. Maximum-likelihood phylogenetic tree based on the alignment of the 18S rRNA gene sequences from *C. malina* (yellow highlighted) and several *Chlamydomonas* strains. Number of branches indicates the percentage of 1000 bootstrap replication supporting a particular node. Black arrows identify the position of *C. malina*, UWO 241 and *C. parkeae* MBIC10599 as closest relatives in the same cluster. A red arrow denotes the position of *C. raudensis* SAG 49.72 in a sister clade. (For interpretation of the references to colour in this figure legend, the reader is referred to the web version of this article.)

0.45  $\mu\text{m}$  pore size fiber glass membrane filter (Milipore). For daily calculation of the biomass concentration ( $W$ ), a calibration curve between the absorbance measured at 750 nm ( $A_{750}$ ) and DCW was established ( $W = 0.884 \cdot A_{750} + 0.0117$ ,  $R^2 = 0.99$ ).

## 2.6. Lipid, protein, and carbohydrate analyses

Total lipids from *C. malina* were extracted using organic solvents, and fatty acid methyl esters (FAMES) from triacylglycerols (TAGs) and polar lipids were identified and quantified by gas chromatography (GC) as previously described by Breuer et al. [24], with some modifications. Briefly, 10 mg of freeze-dried microalgal biomass was weighed using a precision balance (MX5, Mettler-Toledo, USA), then the lipids were extracted and gravimetrically quantified. For the extraction, a mix of chloroform:methanol (2:2.5 v/v) containing an internal standard (Tri-pentadecanoin, C15:0 Triacylglycerol, Sigma-Aldrich, USA) was added to the samples to extract the lipids, and then the cells were disrupted using a bead mill (Bertin technologies, Precellys Evolution, France, 0.1 mm glass beads). Methanol from the solution containing the extracted lipids was separated by adding an aqueous solution of Tris buffer (6 g L<sup>-1</sup> Tris, 58 g L<sup>-1</sup> NaCl, pH 7.5). The chloroform phase containing the lipids was removed and dried under a stream of

nitrogen. To determine the fatty acid composition, lipid samples were chemically derivatized to fatty-acid methyl-esters (FAMES) using 5% H<sub>2</sub>SO<sub>4</sub> in methanol and heated at 70 °C for 3 h. Methanolic H<sub>2</sub>SO<sub>4</sub> from the solution containing the FAMES was separated by adding a mix of hexane:H<sub>2</sub>O (1:1). Finally, samples containing the FAMES and hexane were placed into chromatographic vials. The obtained organic phase was analyzed in a GC fitted with a Flame Ionization Detector (Scienc 436, Bruker, USA) and an Agilent CP-Wax 52 CB column (Agilent Technologies, USA) using splitless injector. To identify and quantify the most common FAMES, external Supelco® 37-component standards (Sigma-Aldrich, USA) were used. Blanks were included in the extraction process to eliminate background trace peaks.

For carbohydrate determination, samples were hydrolyzed with HCl to yield simple sugars, and the resultant monosaccharides were quantified using the phenol-sulphuric acid method [25].

For protein determination, lysis buffer (60 mM Tris pH 9, 2% sodium dodecyl sulfate) was added to 10 mg of freeze-dried biomass samples prior to cells disruption in bead milling system as described before, and then protein content was determined using the Lowry method [26].

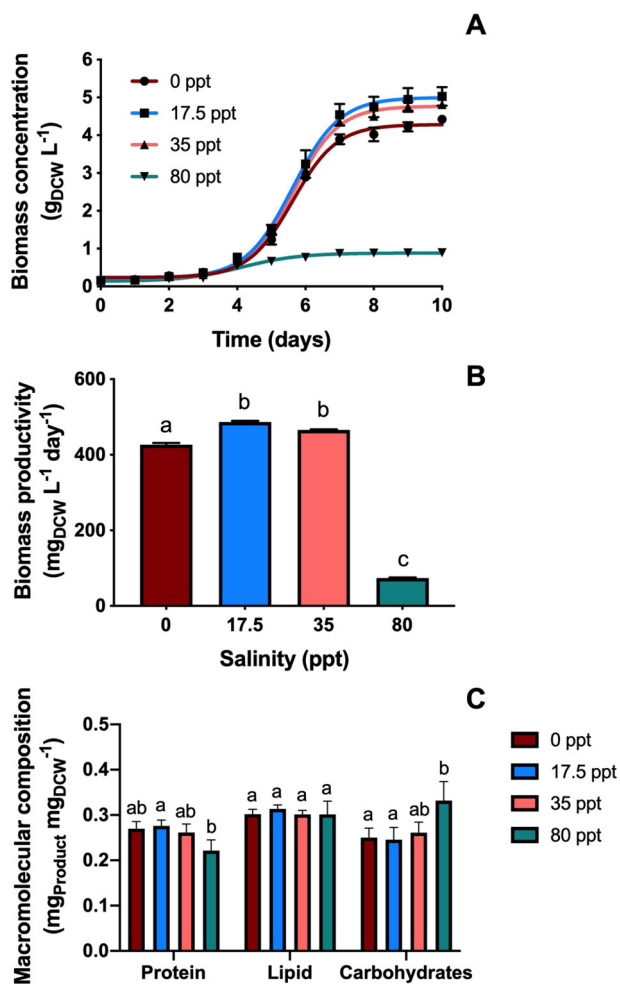


Fig. 2. Effect of salinity. Growth kinetics (A) and biomass productivity (B) of *C. malina* after 10 days of batch cultivation in tubular photobioreactors at  $120 \mu\text{mol photons m}^{-2} \text{s}^{-1}$  in response to salinity concentrations. The macromolecular composition (C) was analyzed in the middle of exponential growth phase (day 5). Values on the Y-axis indicate the mean and standard deviation of three independent experiments. Different lowercase letters indicate a significant difference among means of different groups (one-way ANOVA with *post-hoc* Tukey HSD test,  $p < 0.05$ ).

## 2.7. Calculations

The cellular growth kinetic and productivity were calculated accordingly with a 4-parameter logistic function [23] using the following equation:

$$C_x = \phi_1 + \frac{\phi_2 - \phi_1}{1 + \exp\left(\frac{\phi_3 - t}{\phi_4}\right)} \quad (1)$$

where  $C_x$  is the dry weight ( $\text{g L}^{-1}$ ) at time  $t$  (days),  $\phi_1$  is the lowest asymptote (minimum  $C_x$ ),  $\phi_2$  is the upper asymptote (maximum  $C_x$ ),  $\phi_3$  is  $t$  at  $0.5\phi_2$  (the inflection point), and  $\phi_4$  is the scale parameter [23]. From the previous equation, the volumetric productivity was calculated between two time points, accordingly with Eq. (2):

$$P_i = \frac{C_{x,i} - C_{x,i-1}}{t_i - t_{i-1}} \quad (2)$$

where  $P$  is the productivity ( $\text{g L}^{-1} \text{day}^{-1}$ ),  $C_{x,i}$  and  $C_{x,i-1}$  are the concentrations of the biomass ( $\text{g L}^{-1}$ ) at two time points, and  $t_i$  and  $t_{i-1}$  are the time of cultivation (days).

## 2.8. Statistical analysis

For all treatments, the normal distribution of data was confirmed using Shapiro-Wilk test, and the homogeneity of the variance between treatments was validated using Brown-Forsythe test. For salinity and light intensity treatments, one-way analysis of variance (ANOVA) and *post-hoc* Tukey's multiple comparison test were used. For nitrogen stress treatments, a *t*-test was applied.  $P$  values smaller than 0.05 were considered statistically significant.

## 3. Results and discussion

### 3.1. Phylogenetic analysis

Previous results indicated that *C. malina* belongs to the order Chlamydomonales [18], we confirm this result (Fig. S1). We constructed a phylogenetic tree by the comparison of the sequences of 18S rRNA gene of isolate *C. malina* and only the Chlamydomonales order (Fig. 1). In this tree, the *C. malina* strain is placed in a lineage closely related to *C. parkeae*, within the Moewusinia clade. *Chlamydomonas malina* is closely related to *Chlamydomonas* sp. UWO 241 (UWO 241 hereafter, score = 2983 bit, identity = 99%), *Chlamydomonas* sp. SAG 75.94 (score = 2942 bit, identity = 99%) with a strong bootstrap (BS = 100). All the sequences form clusters with bootstrap support of

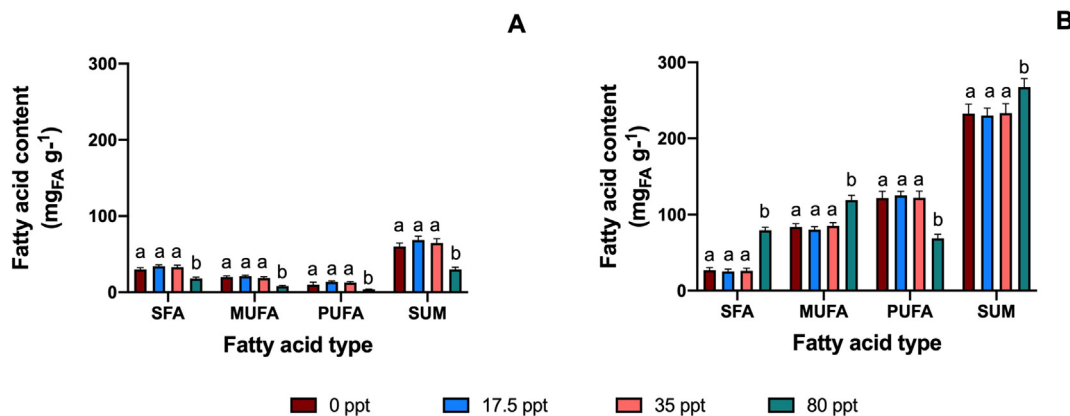


Fig. 3. Effect of salinity on the fatty acid content. Fatty acid content in the polar lipid pool (A) and the TAG pool (B) of *C. malina* at day 5 of batch cultivation at  $120 \mu\text{mol photons m}^{-2} \text{s}^{-1}$  in response to salinity concentrations. SFA: saturated fatty acids, MUFA: monounsaturated fatty acids, PUFA: polyunsaturated fatty acids, TAG: triacylglycerols. Values on the Y-axis indicate the mean and standard deviation of three independent experiments. Statistical comparison was performed individually for each macromolecular component and each class of fatty acid (polar, TAGs, SFA, MUFA, PUFA and sum) among the treatments. Different lowercase letters indicate a significant difference among means of different groups (one-way ANOVA with *post-hoc* Tukey HSD test,  $p < 0.05$ ).

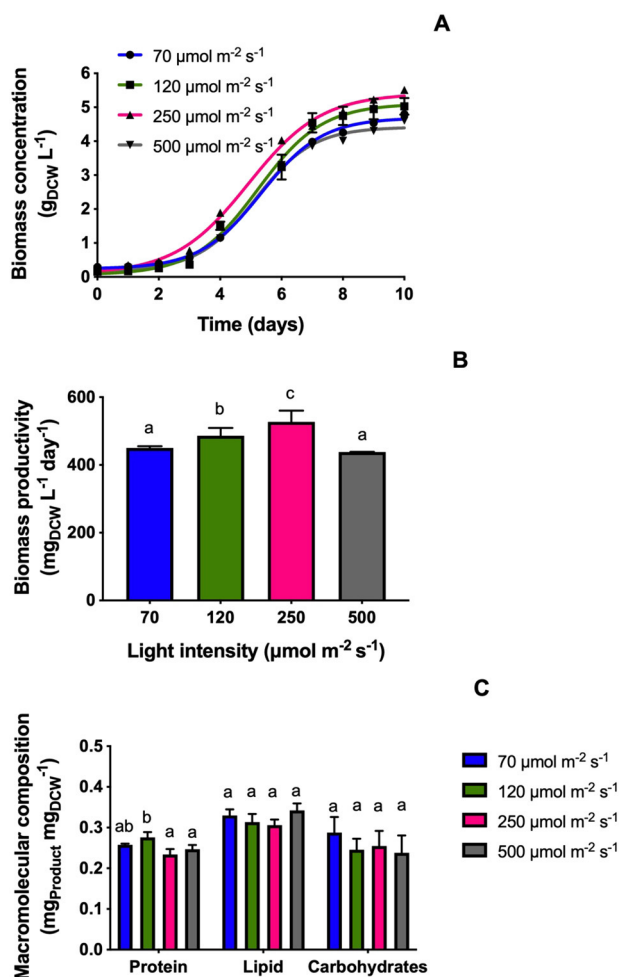


Fig. 4. Effect of light intensity. Growth kinetics (A) and biomass productivity (B) of *C. malina* after 10 days of batch cultivation at a salinity of 17.5 in flat-panel photobioreactors in response to light intensities. The macromolecular composition (C) was analyzed in the middle of exponential growth phase (day 5). Values on the Y-axis indicate the mean and standard deviation of three independent experiments. Different lowercase letters indicate a significant difference among means (one-way ANOVA with *post-hoc* Tukey HSD test,  $p < 0.05$ ).

no less than 50%. Previous phylogenetic studies indicated that this microalga cluster together with *C. raudensis* CCAP 11/131 and *C. parkeae* within the Moewusii clade [18]. It is clear that *C. malina* belongs to the Chlamydomonadales order, mainly composed by freshwater flagellates within the Chlorophyceae [18]. However, *C. malina* in the present phylogenetic analysis appeared more closely related to UWO 241 and *C. parkeae* MBIC10599 than to *C. raudensis* that is being grouped in a sister clade (Fig. 1). The reason for this discrepancy is that UWO 241 was earlier misidentified as *C. raudensis* CCAP 11/131 [27]. But recent studies on phylogenetic analysis of nuclear and plastid DNA sequences revealed that UWO 241 is in fact closely affiliated to the marine strain *C. parkeae* SAG 24.89 and strongly differs from *C. raudensis* SAG 49.72 [28].

### 3.2. Effect of salinity

Highest biomass concentration (5.02 g<sub>DCW</sub> L<sup>-1</sup>) and productivity (480 mg<sub>DCW</sub> L<sup>-1</sup> d<sup>-1</sup>) were attained at salinities of 17.5 and 35 ( $p > 0.05$ , Figs. 2A and B). The growth and maximal biomass concentration decreased 5-fold at the highest salinity tested (80) (Figs. 2A and B). *Chlamydomonas malina* RCC2488 is a marine microalga, originated from the Beaufort Sea located in the Arctic Ocean [18]. There, during late summer when most phytoplankton blooms are occurring, salinities shift between 28 and 32 due to freshwater inflow from rivers and melting ice [18,29,30]. *Chlamydomonas malina* may have adapted to these salinity shifts, explaining the high growth performance at salinities  $\leq 35$ . As demonstrated in *C. malina* closest relative, UWO 241, one possible explanation of the salinity tolerance of *C. malina* is the modulation of the redox signal (redox state of plastoquinone pool), affecting later the expression of genes responsible of high salinity acclimation [15,31]. After 7 days of cultivation, cells entered into stationary phase. This condition, could be due to a limitation or depletion of essential nutrients, inhibitory compounds formation, or high cell densities that cause limited nutrient/gas transfer rates due to mixing issues, and limited light penetration into the cultivation that causes cell self-shading.

Protein content in treatments from 0 to 35 had similar values (26.1–27.6% of DCW,  $p > 0.05$ , Fig. 2C). A lower protein content was found in cells cultivated at salinity 80 as compared to 17.5 ( $p < 0.05$ ), probably as a result of a lower metabolic activity.

The carbohydrate content in cells cultivated at salinity  $\leq 35$  was not statistically different (24.5–26.1% of DCW;  $p > 0.05$ ). Carbohydrate accumulation up to 33.2% of DCW was stimulated by high salinities, resulting in a linear trend from salinities 17.5 to 80 (Fig. S2).

In the case of total lipid content, the statistical analysis (one-way

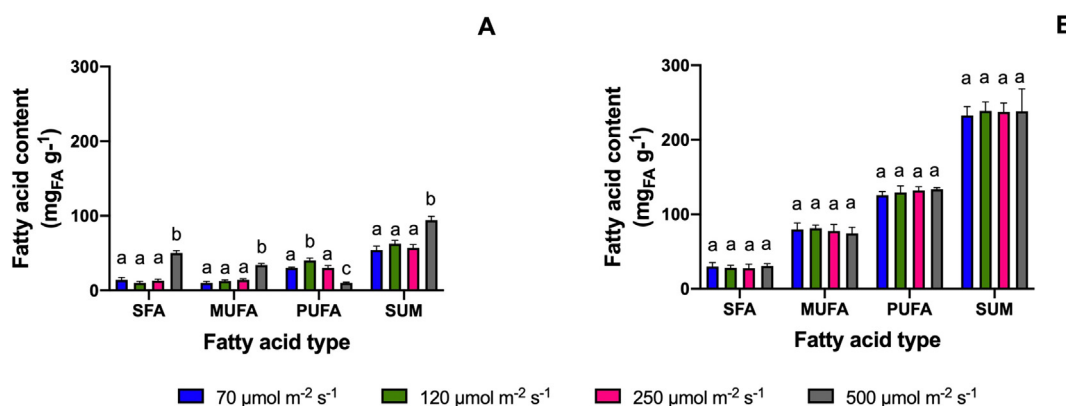
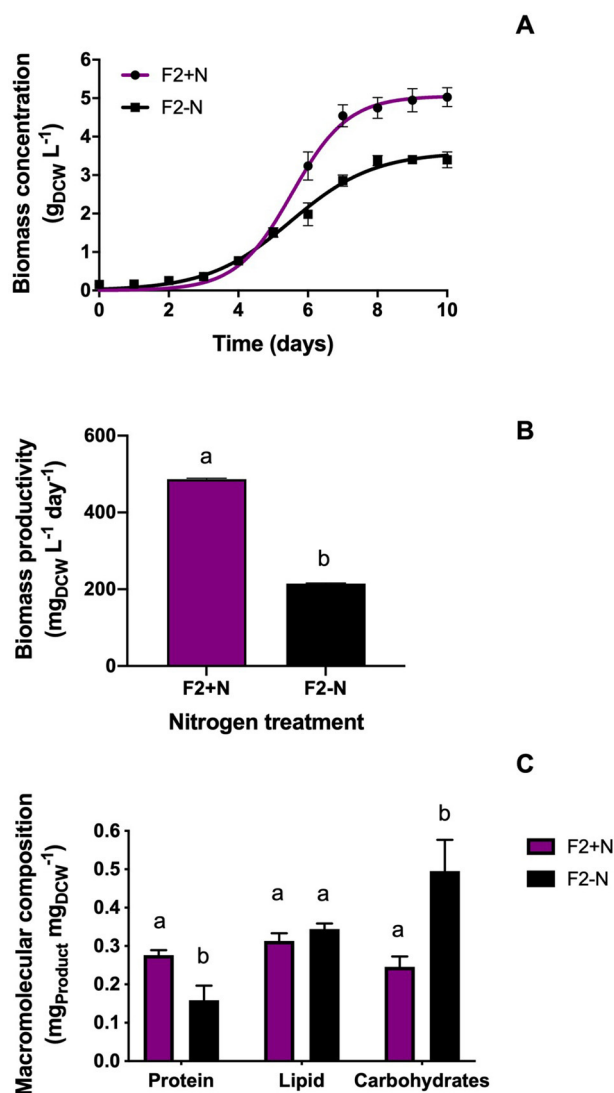


Fig. 5. Effect of light intensity on the fatty acid content. Fatty acid content in the polar lipid pool (A) and the TAG pool (B) of *C. malina* at day 5 of batch cultivation at a salinity of 17.5 in flat-panel photobioreactors in response to light intensities. SFA: saturated fatty acids, MUFA: monounsaturated fatty acids, PUFA: polyunsaturated fatty acids, TAG: triacylglycerols. Values on the Y-axis indicate the mean and standard deviation of three independent experiments. Statistical comparison was performed individually for each macromolecular component and each class of fatty acid (polar, TAGs, SFA, MUFA, PUFA and sum) among the treatments. Different lowercase letters indicate a significant difference among means of different groups (one-way ANOVA with *post-hoc* Tukey HSD test,  $p < 0.05$ ).



**Fig. 6.** Effect of the nitrogen stress. Growth kinetics (A) and biomass productivity (B) of *C. malina* after 10 days of batch cultivation at a salinity of 17.5 and 250  $\mu\text{mol photons m}^{-2} \text{s}^{-1}$  in tubular photobioreactors in response to nitrogen stress. The macromolecular composition (C) analysis was performed after 5 days of nitrogen stress treatments. Values on the Y-axis indicate the mean and standard deviation of three independent experiments. Different lowercase letters indicate a significant difference among means (Student's *t*-test,  $p < 0.05$ ).

ANOVA and *post-hoc* Tukey HSD) demonstrated that there were no significant differences between the salinity treatments. The fatty acid content and class were similar in the treatments at salinities  $\leq 35$  ( $p > 0.05$ , Fig. 3). Cells cultivated at salinities  $\leq 35$  synthesized the double of polar lipids ( $60\text{--}68.5 \text{ mg}_{\text{POLAR LIP}} \text{ g}_{\text{DCW}}^{-1}$ ) than cells grown at salinity 80 ( $30.2 \text{ mg}_{\text{POLAR LIP}} \text{ g}_{\text{DCW}}^{-1}$ ,  $p < 0.01$ , Fig. 3A). In general, the TAG pool comprised the major lipid fraction in all treatments, ranging from 230.1 to 267.4  $\text{mg}_{\text{TAG}} \text{ g}_{\text{DCW}}^{-1}$ . Specifically, into this TAG pool, cells cultivated at salinity  $\leq 35$  mainly synthesized PUFA (hexadecatetraenoic acid, C16:4n-3 and  $\alpha$ -linolenic acid, C18:3n-3) (Fig. 3B and 8A). Maximal PUFA productivity of  $65.1 \text{ mg}_{\text{PUFA}} \text{ L}^{-1} \text{ day}^{-1}$  was obtained in cells cultivated at salinities 17.5 and 35 ( $p < 0.05$ , Fig. 3B). Interestingly, the high biomass productivity at salinity  $\leq 35$  did not compromise the cellular total lipid content as being usually found for microalgae [32,33]. For the ongoing experiments, a salinity of 17.5 was chosen.

### 3.3. Effect of light intensity

The highest biomass concentration of  $5.3 \text{ g L}^{-1}$  and overall productivity of  $527.4 \text{ mg}_{\text{DCW}} \text{ L}^{-1} \text{ day}^{-1}$  was found at 250  $\mu\text{mol photons m}^{-2} \text{s}^{-1}$  ( $p < 0.05$ , Figs. 4A and B). Strikingly, *C. malina* could grow at low but also at high light intensities, suggesting that this microalga may tolerate high light intensities such as 500  $\mu\text{mol photons m}^{-2} \text{s}^{-1}$  or even higher. The ability of *C. malina* to grow at high light intensities was not found in UWO 241, which did not grow above light intensities of 250  $\mu\text{mol photons m}^{-2} \text{s}^{-1}$  [15,34]. Probably, one reason could be that UWO 241 lacks PsbS, which is a protein that plays a key role in photoprotection [31], however the presence of this protein in *C. malina* is unknown. Therefore, for further studies, it would be an interesting phenomenon to investigate the effect of even higher light intensities on the physiology, metabolism, and genome of *C. malina*. Nevertheless, the high performance of *C. malina* in a broad range of light intensities may be a consequence of living in the Arctic, where this microalga had to adapt to low light levels occurring during winter and to high light irradiances during summer [10]. Adaptations to light variabilities include evolution to a structurally and functionally distinct photosynthetic apparatus, and augmented light-harvesting apparatus [10,27]. It has been demonstrated that some polar algae from the genera *Chlamydomonas* and *Chloromonas* are able to produce various secondary carotenoids, such as astaxanthin when they are exposed to high light conditions [12,35]. These carotenoids are known to play a role in stress response such as shielding the photosystem against excessive irradiation [36]. Consequently, a detailed study of pigments content in *C. malina* is suggested. After 7 days of cultivation, cells entered into stationary phase, possibly due to the effects previously mentioned in Section 3.2.

The highest protein content was found in the treatments at 70 and 120  $\mu\text{mol m}^{-2} \text{s}^{-1}$  (27.6% of DCW,  $p = 0.2325$ , Fig. 4C).

The content of carbohydrate and lipid had no significant differences ( $p > 0.05$ ) among all light intensities, suggesting that light intensities, ranging from 70 to 500  $\mu\text{mol photons m}^{-2} \text{s}^{-1}$ , did not have an effect on the synthesis of energy reserve metabolites in *C. malina*. This response is contradictory to what has been observed with other microalgal strains. For example, diminution of the protein and carbohydrate content but an increase in the lipid content are typical responses to high light intensity in several strains [37–41]. Nevertheless, in all treatments the lipid and carbohydrate content were relatively high for cells taken in the mid exponential phase of growth. As discussed below, probably another stressor, such as temperature, induced high lipid and carbohydrate synthesis. The highest light intensity (500  $\mu\text{mol photons m}^{-2} \text{s}^{-1}$ ) induced higher content of polar lipids ( $p < 0.01$ ; Fig. 5A), specifically SFA (C14:0, C16:0 and C18:0; Fig. 8B) and MUFA (C16:1n-7, C18:1n-9, C18:1n-7; Fig. 8B). This increase in the polar lipids pool was probably due to remodeling or relocation of membrane lipids in response to the high light intensity [39,42,43]. For example, the glycolipid digalactosyl diacylglycerol (DGDG) is known to stabilize, structurally and functionally, the chloroplast which led to cell survival [39,42,43]. Photoprotection is another function of polar lipids like monogalactosyl diacylglycerol (MGDG) at high light intensities [39,42,43]. Indeed, high levels of membrane lipids were also found in UWO 241 (*C. malina* closest relative), where polar lipids were mainly composed of MGDG, DGDG, and sulfoquinovosyldiacylglycerol [31]. In all treatments, lipids were mainly TAG with similar composition (Fig. 5B;  $p > 0.05$ ). This TAG fraction comprises primarily of PUFA such as C16:4n-3 and C18:3n-3 (Fig. 8B). The maximal total PUFA productivity of  $83.8 \text{ mg}_{\text{PUFA}} \text{ L}^{-1} \text{ day}^{-1}$  was found in the treatments at light intensities of 120 and 250  $\mu\text{mol photons m}^{-2} \text{s}^{-1}$  ( $p > 0.05$ ).

### 3.4. Nitrogen stress

Nitrogen stress condition was applied to *C. malina* cells to test if energy reserve metabolites can be accumulated. Due to a halt in cell

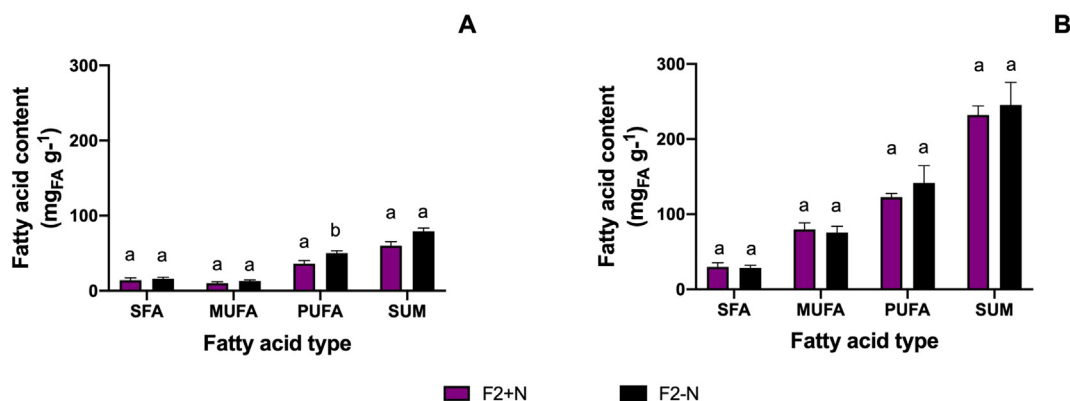


Fig. 7. Effect of nitrogen stress on the fatty acid content. Fatty acid content in the polar lipid pool (A) and the TAG pool (B) of *C. malina* after 10 days of batch cultivation at a salinity of 17.5 and 250  $\mu\text{mol photons m}^{-2}\text{s}^{-1}$  in tubular photobioreactors in response to nitrogen stress. SFA: saturated fatty acids, MUFA: monounsaturated fatty acids, PUFA: polyunsaturated fatty acids, TAG: triacylglycerols. Values on the Y-axis indicate the mean and standard deviation of three independent experiments. Statistical comparison was performed individually for each macromolecular component and each class of fatty acid (polar, TAGs, SFA, MUFA, PUFA and sum) among the treatments. Different lowercase letters indicate a significant difference among means (Student's *t*-test,  $p < 0.05$ ).

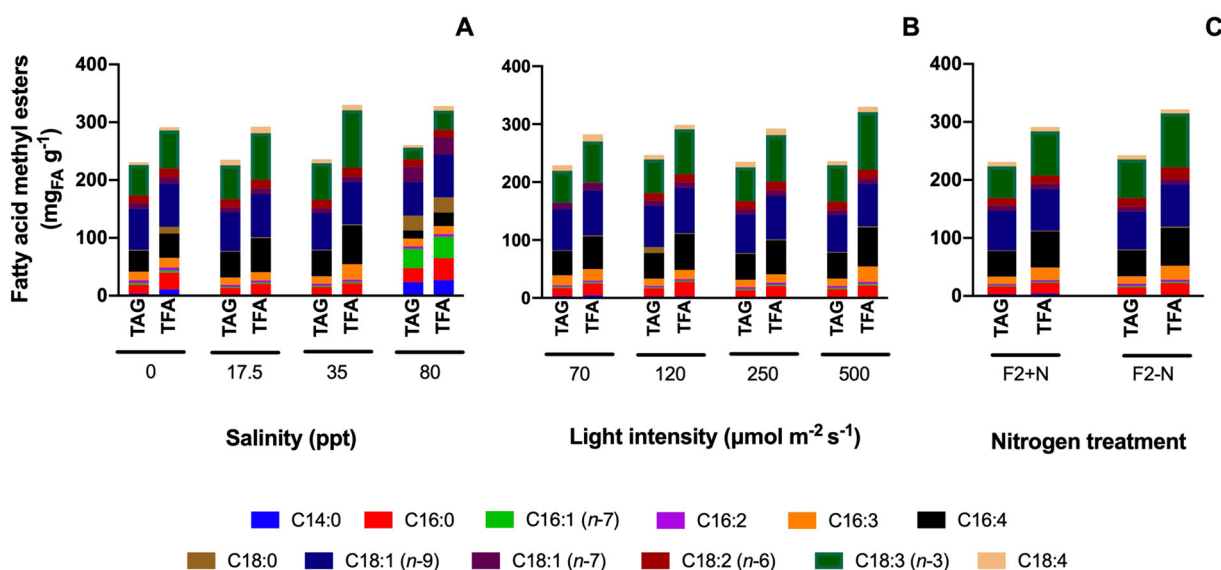


Fig. 8. Fatty acid profiles in the different treatments. Effect of salinity (A), light intensity (B) and nitrogen stress (C) treatments on the fatty acid profile of total fatty acids (TFA) and fatty acids in triacylglycerols (TAG) contained in *C. malina* cells. Values on the Y-axis indicate the mean and standard deviation of three independent experiments.

division, the final biomass concentration and productivity of cells maintained under nitrogen deprivation (F2–N) were  $\sim 2$  times lower than cultures at replete nitrogen conditions (F2 + N, Figs. 6A and B,  $p < 0.0001$ , *t*-test). Cells reached stationary phase after one day under nitrogen deplete conditions and after two days under nitrogen replete conditions. Possibly causes are described in Section 3.2. Nitrogen deprivation stimulated the accumulation of carbohydrates (up to 49.5% DCW,  $p < 0.01$ , *t*-test, Fig. 6C), at protein synthesis expenses (12% DCW decrease,  $p < 0.01$ , Fig. 6C). One of the most preferred strategies to increase reserve metabolites production in several microalgal species is a nutrient stress, like nitrogen deprivation [44]. When nitrogen availability is limited, cells synthesize energy storage compounds such as carbohydrates, while reducing nitrogen-containing compounds such as proteins [45]. Hence, this strategy was effective for carbohydrate but not for lipid accumulation. The lipid content had no significant differences among the treatments ( $p > 0.05$ ; Fig. 6C). Nevertheless, the lipid content of *C. malina* is relatively high in both treatments (average 32.5% of DCW), compared with other *Chlamydomonas* strains, such as the mesophilic *C. reinhardtii*, that can accumulate up to 19% at nutrient replete conditions [46]. This high lipid content has been reported in

other polar and mesophilic algal species as an essential player for temperature acclimation and adaptation [47–49]. Consequently, a possible explanation is that this polar algal strain was already under a temperature stress at 8 °C, which induced lipid accumulation in all treatments tested in this study. Although, we advise additional studies at lower temperatures to support this observation. The total PUFA productivity of cells cultivated in F2 + N was 76.9  $\text{mg}_{\text{PUFA}} \text{L}^{-1} \text{day}^{-1}$ , while the PUFA productivity of cells maintained in F2–N was substantially lower (40.9  $\text{mg}_{\text{PUFA}} \text{L}^{-1} \text{day}^{-1}$ ). In both cases, PUFA was mainly comprised of C16:4*n*-3 and C18:3*n*-3 (Fig. 8C). The proportion of total polar lipids and total TAG was similar in both treatments ( $p > 0.05$ , Figs. 7 and 8C). The PUFA content in the TAG pool (Fig. 7B) was similar in F2 + N and F2–N ( $p > 0.05$ ). However, the PUFA content in the polar lipid pool was significantly higher in F2–N ( $p < 0.05$ ) (Figs. 7A and 8C). The effect of low temperature on the membrane lipid composition is well-known [50,51], like the contribution of C16:4*n*-3 in the transition from liquid-crystalline to gel phase [31]. This phenomenon has been also observed in the psychrophilic UWO 241, which contains high levels of C16:4*n*-3 [52]. Nevertheless, the combined effect of low temperature and nitrogen deprivation on the

membrane lipid composition is not yet understood and requires further studies.

### 3.5. *Chlamydomonas malina* for biotechnology

Currently, commercial microalgal production is limited to mesophilic organisms with optimal temperature productivities of around 24–40 °C [16,53–56]. However, in colder climates, this approach is unfeasible due to higher production cost inherent to energy expenses for heating or seasonal production times limited to summer months. In addition, we found that some microalgae have a high productivity and are rich in omega-3 fatty acids [16]. In this context, polar and cold-adapted microalgae, such as *C. malina*, are efficient alternatives for biomass and metabolite production in cold climates [9,16]. In the present study, we optimized the cultivation of a polar microalga. Our results indicate that the biomass productivities obtained from *C. malina* are comparable with the biomass productivities of mesophilic and other polar and cold-adapted microalgae [9,16,44]. It is noteworthy that the metabolic rates (measured here as biomass productivity) of polar and cold-adapted microalgae were not reduced due to low temperatures, as suggested by several studies [57–59]. This statement probably is only applicable to mesophilic microalgae that cannot grow below thermal optimum temperature [16]. Taken together, optimized *C. malina* can be potentially employed for cultivation in cold climates with high biomass productivities. The metabolites produced by *C. malina* have the potential to be used in biotechnological applications. For example, PUFA are essential nutrients for a balanced human and animal diet, and their nutraceutical and pharmaceutical applications have been extensively reviewed [60–62]. Biofuels can be produced from neutral lipids (TAGs) and carbohydrates [8,63,64]. Proteins from *C. malina* can be marketed as human health food or as animal feed [65–68], but prior protein quality analysis is suggested. Further studies to determine a possible production of high-value pigments, like lutein and astaxanthin from *C. malina*, would be desired and recommended to evaluate the potential use of this strain in food, nutraceutical, pharmaceuticals and cosmetics applications [69–72], among others.

### 4. Conclusions

The arctic green alga *Chlamydomonas malina* RCC2488 is a novel polar microalga that belongs to the Chlamydomonadales order, closely related to the well-studied Antarctic strain *Chlamydomonas* sp. UWO 241. Both strains share similar physiological features such as tolerance to a wide range of salinities, high lipid content composed mainly by C16:4n-3 and C18:3n-3. However, *C. malina* tolerate high light intensities, a trait that was not found for UWO 241. *Chlamydomonas malina* achieved maximum productivities of biomass (527 mg L<sup>-1</sup> day<sup>-1</sup>), lipids (161.3 mg L<sup>-1</sup> day<sup>-1</sup>) and PUFA (85.4 mg L<sup>-1</sup> day<sup>-1</sup>) under nitrogen replete conditions at salinity 17.5 and a light intensity of 250 μmol photons m<sup>-2</sup> s<sup>-1</sup>. Nitrogen deprivation triggered the accumulation of carbohydrates in cells (up to 49.5% w/w) at the expense of proteins but without compromising lipid biosynthesis. *Chlamydomonas malina* is a polar microalga suitable for biomass, lipid, PUFAs and carbohydrate production at 8 °C with potential biotechnological applications.

### Author contributions

Rene Wijffels designed the research in the workpackage in the A2F project which resulted in this manuscript. Based on that framework Daniela Morales-Sánchez designated the study and collected the data. Daniela Morales-Sánchez and Peter Schulze performed the bioreactor experiments and executed lipid and fatty acid analysis. Daniela Morales-Sánchez, Peter Schulze, Rene Wijffels and Kiron Viswanath contributed to manuscript drafting, discussion and critical revision of the article for important intellectual content.

### Funding

This work was funded by the Research Council of Norway's BIONÆR Programme and is part of the Algae2Future project (267872).

### Declaration of competing interest

The authors declare that the research was conducted in the absence of any commercial or financial relationships that could be construed as a potential conflict of interest. No conflicts, informed consent, or human or animal rights are applicable to this study.

### Appendix A. Supplementary data

### References

- [1] C.H.S. Ruxton, S.C. Reed, M.J.A. Simpson, K.J. Millington, The health benefits of omega-3 polyunsaturated fatty acids: a review of the evidence, *J. Hum. Nutr. Diet.* 17 (2004) 449–459, <https://doi.org/10.1111/j.1365-277X.2004.00552.x>.
- [2] I. Khozin-Goldberg, U. Iskandarov, Z. Cohen, LC-PUFA from photosynthetic microalgae: occurrence, biosynthesis, and prospects in biotechnology, *Appl. Microbiol. Biotechnol.* 91 (2011) 905–915, <https://doi.org/10.1007/s00253-011-3441-x>.
- [3] D.A. Martins, L. Custódio, L. Barreira, H. Pereira, R. Ben-Hamadou, J. Varela, K.M. Abu-Salah, Alternative sources of n-3 long-chain polyunsaturated fatty acids in marine microalgae, *Mar. Drugs*. 11 (2013) 2259–2281, <https://doi.org/10.3390/md11072259>.
- [4] F. Guihéneuf, D.B. Stengel, LC-PUFA-enriched oil production by microalgae: accumulation of lipid and triacylglycerols containing n-3 LC-PUFA is triggered by nitrogen limitation and inorganic carbon availability in the marine haptophyte *Pavlova lutheri*, *Mar. Drugs*. 11 (2013) 4246–4266, <https://doi.org/10.3390/md11114246>.
- [5] J. Greene, S.M. Ashburn, L. Razzouk, D.A. Smith, Fish oils, coronary heart disease, and the environment, *Am. J. Public Health* 103 (2013) 1568–1576, <https://doi.org/10.2105/AJPH.2012.300959>.
- [6] M.E. De Swaaf, L. Sijtsma, J.T. Pronk, High-cell-density fed-batch cultivation of the docosahexaenoic acid producing marine alga *Cryptocodinium cohnii*, *Biotechnol. Bioeng.* 81 (2003) 666–672, <https://doi.org/10.1002/bit.10513>.
- [7] D. Morales-Sánchez, O.A. Martínez-Rodríguez, A. Martínez, Heterotrophic cultivation of microalgae: production of metabolites of commercial interest, *J. Chem. Technol. Biotechnol.* 92 (2017) 925–936, <https://doi.org/10.1002/jctb.5115>.
- [8] R.H. Wijffels, M.J. Barbosa, An outlook on microalgal biofuels, *Science* (80-. ) 329 (2010) 796–799, <https://doi.org/10.1126/science.1189003>.
- [9] H. Suzuki, C.J. Hulatt, R.H. Wijffels, V. Kiron, Growth and LC-PUFA production of the cold-adapted microalga *Koliella antarctica* in photobioreactors, *J. Appl. Phycol.* (2018) 1–17, <https://doi.org/10.1007/s10811-018-1606-z>.
- [10] R.M. Morgan-Kiss, J.C. Prisco, T. Pocock, L. Gudyňaite-Savitch, N.P.A. Huner, Adaptation and acclimation of photosynthetic microorganisms to permanently cold environments, *Microbiol. Mol. Biol. Rev.* 70 (2006) 222–252, <https://doi.org/10.1128/MMBR.70.1.222-252.2006>.
- [11] T. Řezanka, L. Nedbalová, K. Sigler, Unusual medium-chain polyunsaturated fatty acids from the snow alga *Chloromonas brevispina*, *Microbiol. Res.* 163 (2008) 373–379, <https://doi.org/10.1016/j.micres.2006.11.021>.
- [12] T. Leya, A. Rahn, C. Lütz, D. Remias, Response of arctic snow and permafrost algae to high light and nitrogen stress by changes in pigment composition and applied aspects for biotechnology, *FEMS Microbiol. Ecol.* 67 (2009) 432–443, <https://doi.org/10.1111/j.1574-6941.2008.00641.x>.
- [13] B. Lyon, T. Mock, Polar microalgae: new approaches towards understanding adaptations to an extreme and changing environment, *Biology (Basel)* 3 (2014) 56–80, <https://doi.org/10.3390/biology3010056>.
- [14] A. Lomsadze, D.D. Dunigan, T. Pröschold, J. Pangilinan, A. Salamov, J. Schmutz, J.-M. Claverie, M. Borodovsky, A. Brueggeman, T. Yamada, A. Kuo, S. Lucas, J. Gunton, D. Weeks, E. Lindquist, I.V. Grigoriev, I. Agarkova, I. Ladunga, J.L. Van Etten, G. Blanc, J. Grimwood, The genome of the polar eukaryotic microalga *Coccomyxa subellipsoidea* reveals traits of cold adaptation, *Genome Biol.* 13 (2012) R39, <https://doi.org/10.1186/gb-2012-13-5-r39>.
- [15] T. Pocock, A. Vetterli, S. Falk, Evidence for phenotypic plasticity in the Antarctic extremophile *Chlamydomonas raudensis* Ettl. UWO 241, *J. Exp. Bot.* 62 (2011) 1169–1177, <https://doi.org/10.1093/jxb/erq347>.
- [16] C.J. Hulatt, O. Berec, E.S. Egeland, R.H. Wijffels, V. Kiron, Polar snow algae as a valuable source of lipids? *Bioresour. Technol.* 235 (2017) 338–347, <https://doi.org/10.1016/j.biortech.2017.03.130>.
- [17] S.C.P. Schulze, C. Hulatt, D. Morales-Sánchez, R. Wijffels, V. Kiron, Fatty acids and proteins from marine cold adapted microalgae for biotechnology, *Algal Res.* 42 (2019) 101604.
- [18] S. Balzano, P. Gourvil, R. Siano, M. Chanoine, D. Marie, S. Lessard, D. Sarno, D. Vault, Diversity of cultured photosynthetic flagellates in the northeast Pacific and Arctic Oceans in summer, *Biogeosciences*. 9 (2012) 4553–4571, <https://doi.org/10.5194/bg-9-4553-2012>.





- future direction, *Mar. Drugs*. 17 (2019), <https://doi.org/10.3390/md17110640>.
- [71] S.P. Cuellar-Bermudez, I. Aguilar-Hernandez, D.L. Cardenas-Chavez, N. Ornelas-Soto, M.A. Romero-Ogawa, R. Parra-Saldivar, Extraction and purification of high-value metabolites from microalgae: essential lipids, astaxanthin and phycobiliproteins, *Microb. Biotechnol.* 8 (2015) 190–209, <https://doi.org/10.1111/1751-7915.12167>.
- [72] K.J.M. Mulders, P.P. Lamers, D.E. Martens, R.H. Wijffels, Phototrophic pigment production with microalgae: biological constraints and opportunities, *J. Phycol.* 50 (2014) 229–242, <https://doi.org/10.1111/jpy.12173>.